LETTER • OPEN ACCESS

The sudden stratospheric warming in January 2021

ENVIRONMENTAL RESEARCH
LETTERS

LETTER

The sudden stratospheric warming in January 2021

Qian Lu[1,2,3], Jian Rao[1,*], Zhuoqi Liang[1], Dong Guo[1], Jingjia Luo[1], Siming Liu[4], Chun Wang[1] and Tian Wang[1]

[1] Key Laboratory of Meteorological Disaster of Ministry of Education, Joint International Research Laboratory of Climate and Environment Change, Collaborative Innovation Center on Forecast and Evaluation of Meteorological Disasters, Institute for Climate and Application Research (ICAR), Nanjing University of Information Science and Technology, Nanjing, Jiangsu 210044, People's Republic of China
[2] Key Laboratory of Meteorology and Ecological Environment of Hebei Province, Shijiazhuang, Hebei 050021, People's Republic of China
[3] Chengde Meteorological Service of Hebei Province, Chengde, Hebei 067000, People's Republic of China
[4] Department of the Geophysical Sciences, University of Chicago, Chicago, IL 60637, United States of America
[*] Author to whom any correspondence should be addressed.

E-mail: raojian@nuist.edu.cn

Keywords: sudden stratospheric warming (SSW), planetary waves, sea ice loss, cold air outbreak

OPEN ACCESS

RECEIVED
30 March 2021

REVISED
4 July 2021

ACCEPTED FOR PUBLICATION
9 July 2021

PUBLISHED
28 July 2021

Abstract

Using the ERA5 reanalysis, sea surface temperature and sea ice observations, and the real-time multivariate Madden–Julian index, this study explores a sudden stratospheric warming (SSW) in January 2021, its favorable conditions, and the near surface impact. Wavenumbers 1 and 2 alternately contributed to the total eddy heat flux from mid-December 2020 to late January 2021, and the wavenumber 2 during the onset period nearly split the stratospheric polar vortex. In mid-December 2020 and during the 2021 New Year period (1–5 January 2021), a blocking developed over the Urals, which enhanced the local ridge and the climatological wavenumber 2. Composite results confirm that the Arctic sea ice loss in autumn and La Niña favor the deepening of the high latitude North Pacific low and the increase of the Urals height ridge, which together enhance the planetary waves and hence disturb the stratospheric polar vortex. However, the Madden–Julian oscillation (MJO) in the tropics was dormant in mid-to-late December 2020 and early January 2021, and the well-established statistical relationship between the MJO convection over the western Pacific and the SSW is not applicable to this special case. The cold air outbreak in China during the 2021 New Year period before the January 2021 SSW onset is not explained by the SSW signal which developed in the stratosphere. In contrast, the downward-propagating signal reached the near surface in mid-February 2021, which may contribute to the cold air outbreak in US and may help to explain the extreme coldness of Texas in middle February.

1. Introduction

On average, sudden stratospheric warming (SSW) occurs 6 or 7 times every decade in the Arctic stratosphere (Cao *et al* 2019, Liu *et al* 2019, Rao *et al* 2019b, 2021). The model evidence has confirmed that the SSWs might increase with global warming, but such an increase is insignificant (Ayarzagüena *et al* 2018, 2020). Arctic stratospheric air temperatures increase by 40–60 K within a week, and in a major SSW the circumpolar jet reverses to easterlies (Charlton and Polvani 2007, Hu *et al* 2014, Butler *et al* 2015, Rao *et al* 2018). The weakening and distortion of the Arctic polar vortex during the SSW is projected onto the negative phase of the Northern Annular Mode/Arctic Oscillation (NAM/AO) (Baldwin and Dunkerton 1999, 2001), which tends to propagate downward and can affect the near surface. Therefore, SSW events can serve to improve the near surface predictability associated with the negative phase of the AO (Karpechko *et al* 2018).

In the last three years, both the Antarctic and Arctic polar stratospheres witnessed a huge variation in their circulation and temperature. Specifically, two major SSWs were observed over the Arctic stratosphere in February 2018 and January 2019, respectively (Karpechko *et al* 2018, Lee and Butler 2019, Rao *et al* 2019a, Lu *et al* 2021). The February 2018 SSW has been reported to be triggered by the blocking in the Urals and Alaska, which disrupt the zonal circulation

in mid-to-high latitudes and amplify the climatological wave amplitudes (Rao *et al* 2018, Overland *et al* 2020). The January 2019 SSW occurred under several favorable conditions, including the solar minima, easterly winds of the quasi-biennial oscillation (QBO), moderate El Niño, and active convection over the marine continent and western Pacific during the Madden–Julian Oscillation (MJO) phase 6 by enhancing upward propagation of extratropical planetary waves (Rao *et al* 2019a). The different configurations of the favorable conditions (Karpechko *et al* 2018, Rao *et al* 2019a, 2020a) and morphologies of the polar vortex (Butler *et al* 2020) for the February 2018 and January 2019 SSWs explain their different predictability, with the latter having greater predictability with a longer lead time than the former in most subseasonal to seasonal forecast systems.

Compared to the NH, very few SSWs take place in the SH due to weaker planetary waves, owing to the even distribution of oceanic water in high latitudes of the SH. Hitherto, only two SSWs (i.e. September 2002 and 2019) have been observed in the SH (Hu 2020, Shen *et al* 2020, Rao *et al* 2020b). Although no SSW event was observed in the 2019/20 boreal winter, an extremely strong stratospheric polar vortex coupled with Arctic ozone loss appeared in March 2020 (Rao and Garfinkel 2020, 2021b).

The 2020/21 winter was very different, with a major SSW on 5 January, attracting wide attention in the media (Lee 2021 and references therein). However, tropospheric precursors for this SSW are not widely explored in literature, and favorable conditions triggering this event are not yet clearly understood either. Not all SSWs show a successful downward propagation of the negative NAM/AO signal from the stratosphere to the troposphere (Karpechko *et al* 2017), so the relationship between the SSW and the near surface predictability is still uncertain. The January 2021 warming event adds another case to the limited sample of historical SSWs, which provides an additional opportunity for studying the downward propagation of the stratospheric SSW signal and its impact on the near surface. The general characteristics of this SSW deserve special report and careful study.

The structure of the paper is organized as follows. Following the introduction, data and methods are described in section 2. Section 3 displays the evolution of the circulation and temperature anomalies during this SSW. Section 4 explores the possible precursors for this SSW event, and the near surface response is also discussed. Finally, conclusions are summarized in the section 5.

2. Data and methodology

The daily ERA5 reanalysis is used in this study, downloaded at a 1° (latitude) ×1° (longitude) horizontal resolution and 37 pressure levels from 1000 to 1 hPa (Hersbach *et al* 2020). Variables analyzed in this study include the geopotential height (Z), zonal and meridional winds (u, v), and air temperature at pressure levels. The monthly sea ice concentration and sea surface temperature (SST) version 1 from 1979 to 2020 are obtained from the Met Office Hadley Centre, with a horizontal resolution of 1° × 1° (Rayner *et al* 2003). The climatology of those variables is calculated as the long-term mean during 1979–2020. Anomalies refer to the deviations of daily data in 2021 from the climatology.

Given the relationship between the tropical MJO and SSWs (Garfinkel *et al* 2012), the real time multivariate MJO index (Wheeler and Hendon 2004) is used to test the tropical conditions for the January 2021 SSW, which is available from the Australian Bureau of Meteorology (www.bom.gov.au/climate/mjo/graphics/rmm.74toRealtime.txt). Considering that the vertical component (F_z) of the Eliassen–Palm flux is approximately proportional to the transient eddy heat flux (Andrews *et al* 1987), the eddy heat flux ($\overline{v^* T^*}$) is calculated using the daily meridional wind and temperature from the ERA5 reanalysis. The overbar means the zonal average, and the superscript asterisk means the zonal deviation. The area-weighted (i.e. the cosine of latitude) eddy heat flux from 45°–75° N at 100 and 300 hPa is used to denote the planetary waves entering the stratosphere in the extratropics from the tropopause and troposphere (Polvani and Waugh 2004, De La Cámara *et al* 2019). As the zonal deviation of the meridional wind and temperature can be decomposed into different wavenumbers and only planetary waves can propagate upward into the stratosphere (Nishii *et al* 2009), the eddy heat flux components by planetary waves (wavenumbers 1–3) are diagnosed (Rao *et al* 2019a, Butler *et al* 2020).

3. Evolution of the January 2021 SSW

3.1. Evolution of the stratosphere-troposphere coupling

The height-temporal evolutions of the circumpolar zonal wind at 60° N, polar cap temperature anomalies, and polar cap height anomalies are shown in figure 1. Based on the first day when the daily-mean circumpolar westerly was reversed to easterly, a major SSW event occurred in the Arctic stratosphere on 5 January, 2021 (figures 1(a) and (d)). The zonal wind at 60° N/10 hPa (figure 1(d)) oscillated around zero: easterly winds appeared from 5 to 20 January for 14 days (with a 2 days westerly interruption) and 2 days from February 1 to 2 (also see Lee *et al* 2021), much longer than the mean duration of easterlies for all SSWs (i.e. 8 days) (Rao and Garfinkel 2021a). The relatively long persistence time of easterlies during this SSW might reflect a persistent strong dynamical forcing, which overwhelms the nonadiabatic cooling

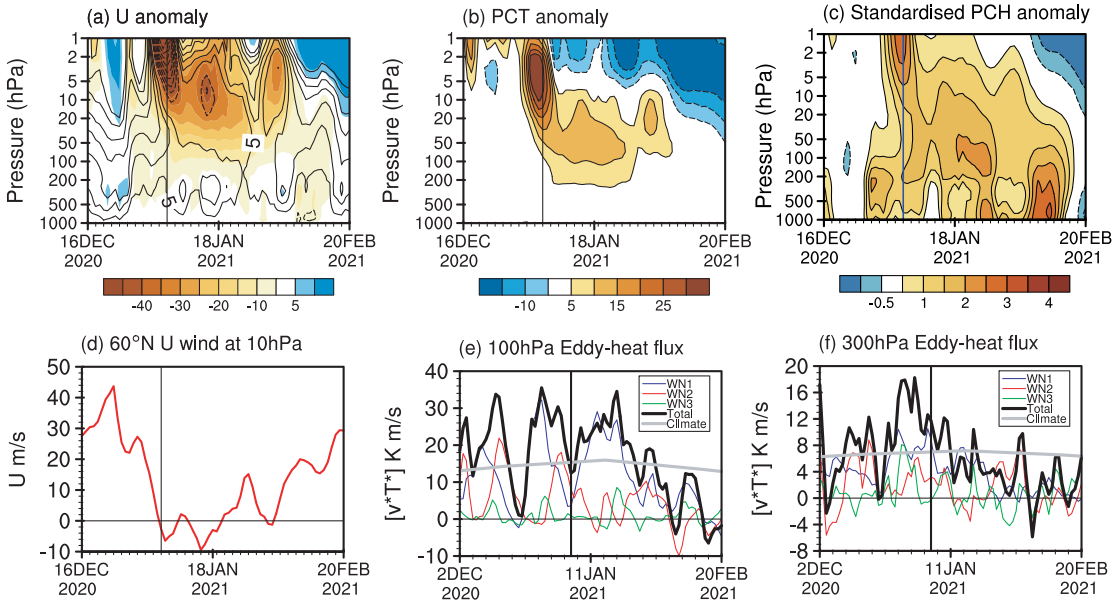

Figure 1. Temporal evolutions of several metrics during 16 December 2020 to 20 February 2021. (a) Zonal-mean zonal wind (contours) and its anomalies (shadings) at 60°N from 1000 to 1 hPa (interval: 5; units: m s^{-1}). (b) Polar cap temperature anomalies area-averaged over 60°–90° N (interval: 5; units: °C). (c) Polar cap height anomalies area-averaged over 60°–90° N scaled by the daily standard deviation in winter (December–February) at each pressure level (interval: 0.5; unitless). (d) Zonal-mean zonal wind at 60° N and 10 hPa (e) eddy heat flux at 100 hPa area-averaged over 45°–75° N by total waves, wavenumber 1 and wavenumber 2 (units: km s^{-1}). (f) As in (e) but for eddy heat flux at 300 hPa. The vertical black line marks the onset date of the SSW.

effect during this period. The daily-mean circumpolar westerlies in the upper stratosphere reversed to easterlies around 31 December 2020 (figure 1(a)). The easterly anomalies formed since 26 December 2020, and they covered a thick vertical extent from 500 hPa to 10 hPa. The easterly anomalies increased rapidly after 3 January 2021 and reach two maxima (−40 m s^{-1}) on 6 and 16 January 2021 above 5 hPa, respectively. The easterly anomalies started on 26 December 2020 and ended on 16 February 2021 at 10 hPa with a persistence time of 53 days.

Consistent with the circumpolar wind evolution, the Arctic stratosphere warms suddenly after 31 December 2020 (anomalies: ∼5 K). The temperature anomalies at 10 hPa developed to the maximum (>25 K) around 4 January 2021, with an abrupt increase of 20 K in five days. Furthermore, the positive temperature anomalies in the polar cap lasted for 38 days throughout 31 December until 6 February 2021 at 10 hPa (figure 1(b)). Warm temperature anomalies primarily developed above 200 hPa. According to the geostrophic wind principle, the reversal of zonal wind is connected with rising of the polar cap geopotential height. Therefore, positive standardized height anomalies were observed to develop several days before the SSW onset and strengthen after the onset. Strong positive geopotential height anomalies were present in both the troposphere and stratosphere after the SSW, with two periods of particularly strong apparent downward propagation: one during 25–31 January and the other during 7–13 February (figure 1(c)). The metric of the standardized polar cap height anomalies is actually a substitute for the NAM index but with the sign reversed (Baldwin and Thompson 2009, Rao *et al* 2020a). In summary, the January 2021 SSW is characterized by its long-lasting time and a possible downward impact.

3.2. Alternate pulses of wavenumber 1 and wavenumber 2

To explain the occurrence of this SSW and compare the contribution by planetary wavenumbers 1 and 2, the eddy heat flux at 100 hPa and 300 hPa area-averaged over 45°–75° N is shown in figures 1(e) and (f). Persistent and long-lasting total eddy heat flux occurred before the onset of the January 2021 SSW, and three peaks should be noted at 100 and 300 hPa (i.e. around 12 December, 27 December and 1 January). Those three pulses are contributed by different planetary waves, with the first peak by wavenumber 2, the second peak by wavenumber 1, and third peak by wavenumber 2 again. Eddy heat flux pulses by wavenumbers 1 and 2 appears alternately, weakening the stratospheric polar vortex persistently. Upward propagation of planetary waves was enhanced before the onset date of this warming event, but such an enhancement did not stop soon after the SSW began. The zonal winds in the troposphere and lower stratosphere were still westerlies and the zero winds were around 50 hPa after the SSW onset. The presence of westerlies in the lower stratosphere denotes a more

baroclinic structure during this SSW (figure 1(a)). Previous studies suggest that the persistence of eddy heat flux is more important for decelerating the zonal mean zonal winds than the strength of the eddy heat flux pulses themselves (Polvani and Waugh 2004). From 5 to 25 January, the total waves in mid-to-high latitudes were still active to produce large eddy heat flux, mainly contributed by wavenumber 1. The strong wave activities especially in the upper troposphere might explain the long-lasting period of this warming event. Therefore, it is reasonably revealed that the onset of this event and its exceptional persistence is due to the alternate dominance of wavenumbers 1 and 2, which still continued after the SSW onset as the westerlies in the lower stratosphere did not reverse soon.

To reveal the variation of the stratospheric polar vortex shape associated with the change in the eddy heat flux pulse in figures 1(e) and (f), the height and its anomalies in the Northern Hemisphere at 10 hPa and 500 hPa during several wave pulse periods are shown in figure 2. The morphology of the stratospheric polar vortex can be disturbed and affected by the tropospheric wave pulses. The first pulse period from 14 to 16 December 2020 was denoted by the elongation of the stratospheric polar vortex toward Arctic Eurasia and Arctic Canada in the stratosphere (two anomalous lows were identified over Arctic Eurasia and Arctic Canada, and an anomalous high developed in the Pacific sector; figure 2(a)) as the tropospheric height anomaly is nearly in phase with the climatological wavenumber 2 (figure 2(d)). In the second stage from 23 to 29 December, the North Pacific high (and its anomaly) center moved slightly westward to Kamchatka Peninsula in the stratosphere (figure 2(b)) while the Aleutian low deepened and the North Atlantic height rose in the troposphere (figure 2(e)). The third stage from 1 to 4 January 2021 was identified with an anomalous wavenumber 2 pattern in the stratosphere (figure 2(c)) and the Urals height rose again in the troposphere (figure 2(f)).

In the fourth stage from 9 to 21 January 2021 the negative height anomalies in midlatitudes are zonally symmetric, indicating the development of the negative NAM in the stratosphere (figure 2(g)); the negative height anomalies over North Pacific and its neighboring area still persisted and intensified the climatological wavenumber 1 in the troposphere (figure 2(j)). In the fifth stage from 23 January to 3 February 2021, the stratospheric polar vortex was still located over the Barents Sea, but with a more circular shape and narrower coverage (figure 2(h)); the tropospheric negative height anomalies over East Asia and North Atlantic, as well as the positive height anomalies over the Urals and Northeast Pacific strengthen the climatological wavenumber 2 (figure 2(k)). In the sixth stage from 6 to 14 February 2021, a gradual recovery of the stratospheric polar vortex was observed (figure 2(i)) as an annular mode response pattern developed in the troposphere (figure 2(l)).

4. Favorable conditions for the January 2021 SSW and its surface impact

4.1. Favorable conditions for occurrence of the January 2021 SSW

Previous studies (Rao *et al* 2019a, Baldwin *et al* 2021) revealed that favorable conditions for occurrence of the NH SSWs include the easterly QBO around 30–50 hPa, moderate El Niño, and solar minimum. However, the 2020/21 winter was not in the easterly QBO phase or in the warm El Niño-Southern Oscillation (ENSO) state; only the solar activities are still during a minimum period of the 11 year cycle (not shown).

Figure 3 displays several metrics that might contribute to the tropospheric variations in January 2021, including ENSO, Arctic sea ice, and the MJO. The January 2021 SSW is preceded by the moderately cold ENSO state (La Niña) in the eastern equatorial Pacific (figures 3(a) and (d)). Statistics in Rao *et al* (2019a) show that both moderate El Niño and La Niña increase the probability of the SSW occurrence compared to the neutral ENSO state. The warm SST anomalies (maximum: ∼2.6 °C) in North Pacific might not explain the strengthening of the Aleutian low in January 2021 (figures 3(d) and (f)), as Hu and Guan (2018) established that warm North Pacific SSTs usually weaken the intensity of the local low center. The coldest SST anomalies in the eastern Pacific can reach −1.8 °C (figure 3(d)), although the area-weighted SST anomaly in the Niño3.4 region is moderately strong (−1.0 °C; figure 3(a)). The composite height anomalies at 500 hPa associated with La Niña is shown in figure 3(g), and 15 La Niña winters for the composite are selected (i.e. the SST anomalies in Niño3.4 region are lower than −0.5 °C for three consecutive wintertime months, November–January; 1984/85, 1985/86, 1989/90, 1996/97, 1999/2000, 2000/01, 2001/02, 2006/07, 2008/09, 2009/10, 2011/12, 2012/13, 2017/18, 2018/19, and 2020/21). A negative Pacific–North American pattern was detected in the La Niña composite, but the positive height anomalies shift equatorward and are not situated over high-latitude North Pacific. It is negative height anomalies that developed over Aleutian Islands (figure 3(g)). Therefore, negative height anomalies over Aleutian Islands are observed during both El Niño and La Niña, implying the asymmetric impact of ENSO on the extratropical circulation (Domeisen *et al* 2019 and references therein). El Niño SST anomalies affect the stratospheric polar vortex by amplifying the wavenumber 1 amplitude, whereas La Niña modulates the vortex by enhancing the wavenumber 2 (Rao *et al* 2019a). Positive height anomalies occupy North Eurasia, further increasing the local climatological ridge.

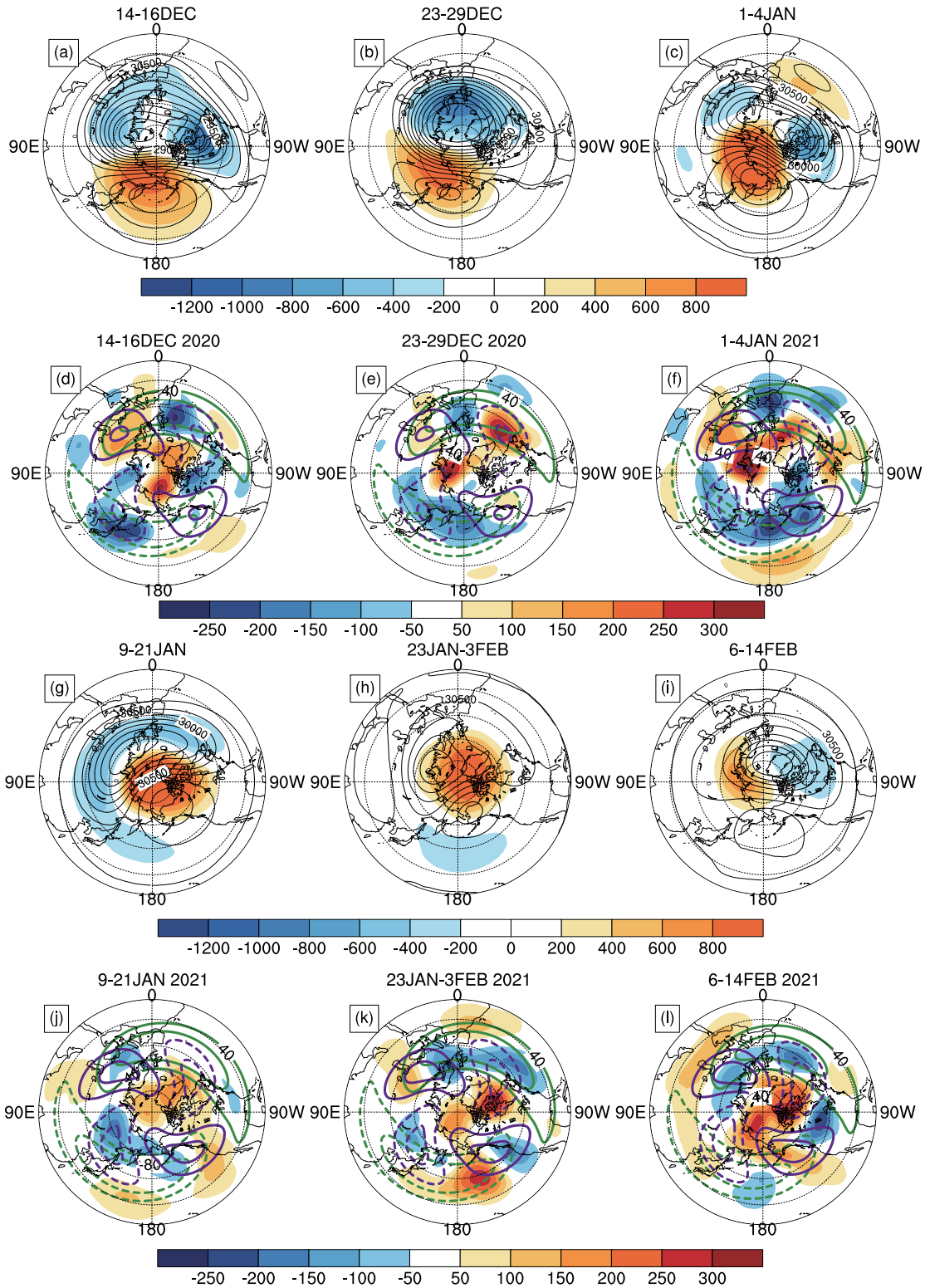

Figure 2. (First and third rows) The 10 hPa height (contours; units: m) and its anomalies (shadings; units: m) and (second and fourth rows) 500 hPa height anomalies (shadings, units: m) in the Northern Hemisphere during different periods alternately dominated by wavenumbers 1 and/or 2. (a), (d) The mean during 14–16 December 2020. (b), (e) The mean during 23–29 December 2020. (c), (f) The mean during 1–4 January 2021. (g), (j) The mean during 9–21 January 2021. (h), (k) The mean during 23 January to 3 February 2021. (i), (l) The mean during 6–14 February 2021. The green and purple contours show the climatological wavenumbers 1 and 2 (units: m), respectively.

In addition, the January 2021 SSW also followed widespread Arctic sea ice loss in autumn (figure 3(e)), particularly over the Barents-Kara Sea (BK, 10°–110° E, 65°–85° N). The detrended autumn Barents-Kara Sea ice density index from 1982 to 2020 is shown in figure 3(b), which is the area-averaged sea ice density over 10°–110° E, 65°–85° N (Screen 2017). In the 2020 autumn, the coverage of

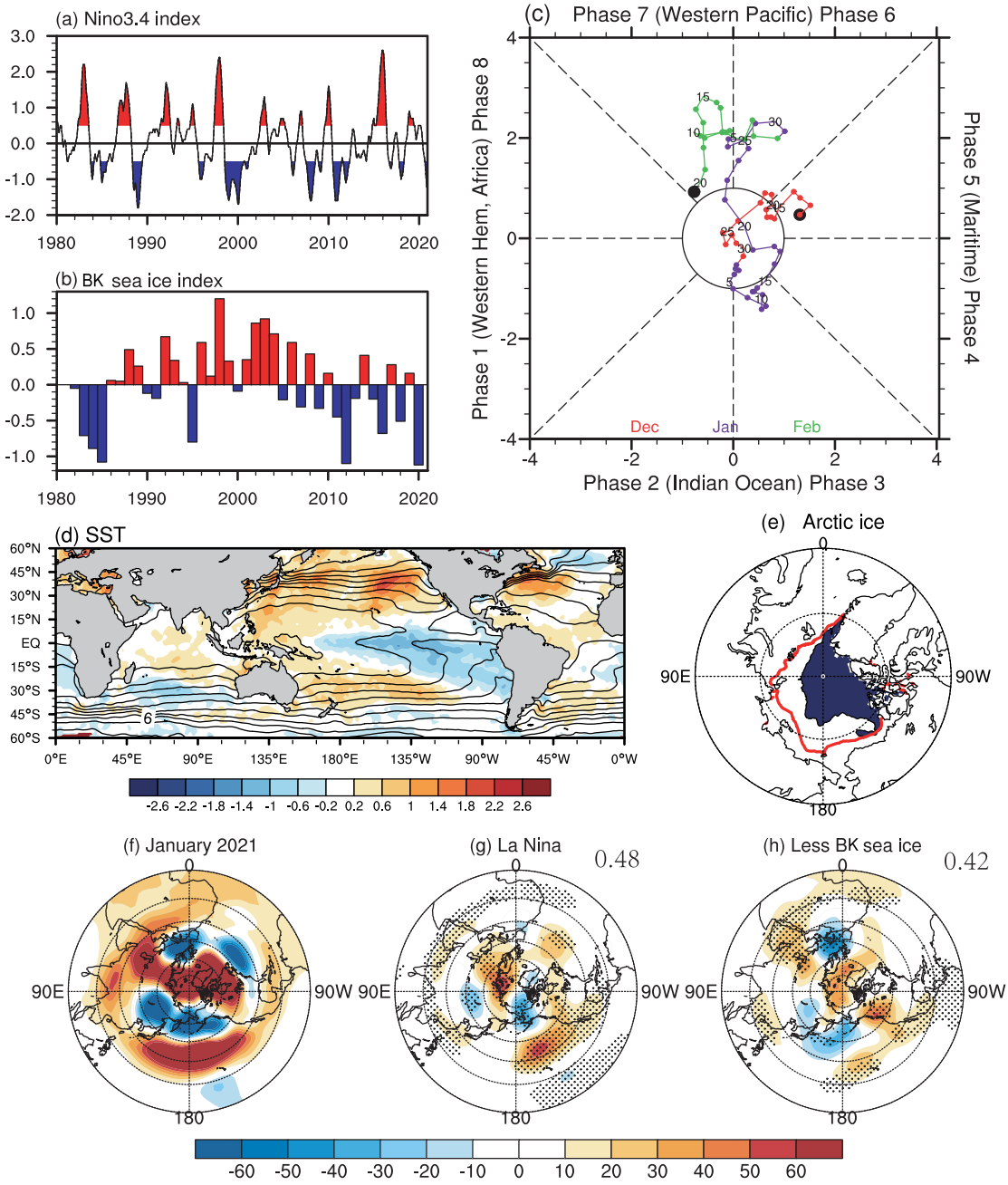

Figure 3. Factors that might contribute to the formation and onset of the January 2021 SSW. (a) The monthly time series of the three-month running mean Niño3.4 (5° S–5° N, 170°–120° W) index (units: °C), which measures the evolution of ENSO. The red (blue) shadings mark the SST anomalies in the Niño3.4 region above 0.5 (below −0.5) °C. (b) Standardised autumn Barents-Kara Sea ice density index from 1982–2020 with the trend removed. (c) Evolution of the tropical MJO from 10 December 2020 to 20 February 2021, represented by the real-time multivariate MJO index. (d) November–December mean SST (contours, units: °C) and its anomalies (shadings, units: °C) in 2020. (e) The distribution of Arctic sea ice in the 2020 autumn (shadings) and the distribution of climatological Arctic sea ice in autumn during 1982–2020 (contours). (f) Synoptic map of the 500 hPa height anomalies in January 2021. (g) Composite height anomalies at 500 hPa in January during La Niña. (h) Composite height anomalies at 500 hPa in January following less Barents-Kara sea ice. Black dots in (g) and (h) indicate the composite height anomalies at the 95% confidence level using the *t* test. The pattern correlation between the composite and the 500 hPa height anomalies in January 2021 is also shown on the top right in (g) and (h).

Barents-Kara Sea ice was significantly reduced. It is reported that sea ice loss in the Barents-Kara Sea during early winter usually strengthens the upward propagation of planetary waves and disturbs the stratospheric polar vortex in January (Kim *et al* 2014, Sun *et al* 2015), although the observed impact of sea ice might be inflated by the effects of atmospheric circulation variability on sea ice (Blackport and Screen 2021). Eight autumns with large Barents-Kara sea ice loss (i.e. the index is lower than -0.5σ) are evident: 1983, 1984, 1985, 1995, 2012, 2016, 2018 and 2020. The composite 500 hPa height anomalies in the following January of heavy Barents-Kara sea ice loss in autumn are shown in figure 3(h), resembling

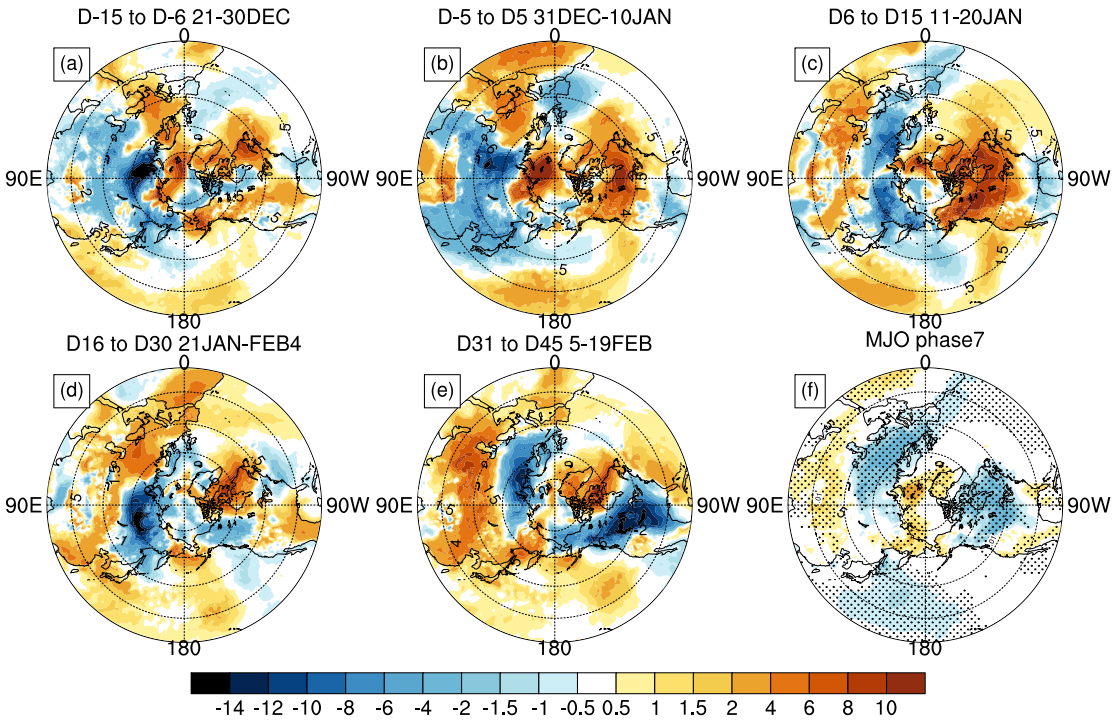

Figure 4. Evolution of the 2 meter temperature (t2m) anomalies during different periods following the January 2021 SSW. (a) The mean t2m anomalies from 21 to 30 December 2020. (b) The mean t2m anomalies from 31 December 2020 to 10 January 2021. (c) The mean t2m anomalies from 11 to 20 January 2021. (d) The mean t2m anomalies from 21 January to 4 February 2021. (e) The mean t2m anomalies from 5 to 19 February 2021. (f) Composite t2m anomalies in winter during the MJO phase 7 (shadings). The dotted region marks the composite at the 95% confidence level.

the observed pattern in January 2021 (figure 3(f)). Namely, the negative height anomalies over North Pacific and positive height anomalies at 500 hPa over Barents-Kara Sea is possibly associated with the Barents-Kara Sea ice loss in the preceding autumn.

In summary, the persisting wave activities in the troposphere from late-December 2020 to late-January 2021 can be associated with the moderate La Niña and the heavy ice loss over the Arctic. In contrast, the MJO was fairly weak within two weeks before the SSW onset (figure 3(c)). The convection over the western Pacific was enhanced during late January and February, much later than the SSW onset (see MJO phases 6 and 7 in figure 3(c)).

4.2. Possible surface impact of the January 2021 SSW

As the zonal-mean signal associated with the SSW propagates downward to the troposphere, the near surface responds (Rao *et al* 2020a, Lu *et al* 2021). Composite results in previous studies (Cao *et al* 2019, Liu *et al* 2019, Rao *et al* 2021) show that the near surface temperature patterns before and after the SSW onset are not the same: cold anomalies form over the Eurasian continent before the SSW onset, while both North Eurasian and North American continents are cold in the following 1–2 month after the SSW onset. The 2 meter temperature (t2m) anomalies are shown in figure 4 during the January 2021 SSW. The composite results in previous studies are still true for the January 2021 SSW event. Namely, in the pre-SSW to onset periods (figures 4(a) and (b)), North Eurasia is anomalously cold, while warm anomalies develop in Canada. The pre-SSW temperature pattern is not likely a response to the stratospheric variation, but a tropospheric variation itself. A nationwide cold surge struck China during the 2021 New Year (figure 4(b)), and the cold anomalies during this period in Asia develop further equatorward than those during 21–30 December (figure 4(a)). The cold air outbreak in China during 31 December–10 January was mainly caused by the development of the Urals blocking, which enhances the meridional circulation in the downstream area, East Asia (see the local positive height anomalies in figure 2(f)).

Within the following month after the SSW onset when the SSW signals mainly developed in the stratosphere and upper troposphere, cold anomalies still persisted in high latitudes of Russia due to tropospheric variability and warm anomalies gradually diminished in large parts of North America (figures 4(c) and (d)). In the second month after the January 2021 SSW onset, the downward-propagating signals seemed to reach the near surface (figure 1). The negative NAM developed at near surface, which had appeared before the SSW onset (figure 1(c)). The extremely cold wave in Texas and the cold air outbreak in US were related to the near surface negative NAM in mid-to-late February (figure 4(e)). The composite MJO phase 7 also corresponds to a significant cold

pattern in Canada and central US (figure 4(f)), which additionally explains the cold anomalies in large parts of the US.

5. Summary

Using the ERA5 reanalysis, the SST and sea ice observations, and the real-time multivariate MJO index, the evolution of the January 2021 SSW event, favorable conditions for the occurrence of this case, and its surface impact are explored in this study. The main conclusions are as follows.

(a) In December 2020, the upward propagation of planetary wave energy progressively accumulated in the extratropical stratosphere, denoted by the alternate wavenumber 1 and wavenumber 2 eddy heat flux pulses. In mid-December 2021, the wavenumber 2 pulse dominated the total eddy heat flux in the circumpolar region. In late-December 2020, the wavenumber 1 forcing strengthened and continued to accumulate the total eddy heat flux. In the 2021 New Year period, the wavenumber 2 redeveloped and the stratospheric polar vortex elongated and possessed two anomalous low centers, and the circumpolar westerlies reversed to easterlies. The persistent alternate wavenumber 1 and wavenumber 2 forcing in December 2020 led to a large stratospheric perturbation. Owing to the continuous wave forcings, the zonal wind deceleration began nearly one week earlier before the SSW onset, and the circumpolar easterly anomalies and negative NAM signal also preceded the SSW onset by nearly one week.

(b) Previous studies show that the composite eddy heat flux decrease rapidly after the SSW onset (Cao *et al* 2019, Liu *et al* 2019, Rao *et al* 2021); in contrast, the wave forcing did not stop after the January 2021 SSW onset. Consistent with the long-lasting period of the eddy heat flux pulse after its onset, this SSW lasted for ∼2 months. After the SSW onset, large negative NAM-like signals propagated downward to the near surface during late-January and mid-February.

(c) In mid-December 2020 and during the 2021 New Year period (1–5 January 2021), enhanced wavenumber 2 was observed to propagate from the troposphere to the stratosphere, explaining the elongation and two anomalous low centers of stratospheric polar vortex. A blocking commonly developed over the Urals in these two periods, which enhances the local ridge and the climatological wavenumber 2. In late December 2020 and during the post-SSW period, an anomalous low appeared over North Pacific, which favors the deepening of the local trough and the climatological wavenumber 1.

(d) Favorable conditions for the occurrence of the SSW in January 2021 include the BK sea ice loss in the preceding autumn and the cold SST state in tropical Pacific (i.e. a La Niña developed in the 2020/21 winter). Composite 500 hPa height anomaly patterns in January for the BK sea ice loss in autumn and La Niña are highly consistent with the observed circulation anomaly in January 2021. Both conditions favor the deepening of the high latitude North Pacific low and the rising of the Urals ridge. In contrast, the tropical convection over western Pacific associated with the MJO phase 6 is fairly weak in the pre-SSW and onset periods.

(e) Cold air outbreak in China during the 2021 New Year period is not solely due to the stratospheric variation, because the SSW signal mainly developed in the stratosphere and did not reach the near surface. This cold surge was mainly related to the synchronous upstream blocking development over the Urals. In contrast, the second downward-propagating signal reached the near surface in middle February 2021, which together with the MJO phase 7 are consistent with the cold air outbreak in the US and associated extreme coldness of Texas in middle February.

Data availability statement

All data that support the findings of this study are included within the article (and any supplementary files).

Acknowledgments

The work of data analysis and paper writing was conducted at Key Laboratory of Meteorological Disaster, Ministry of Education in Nanjing University of Information Science and Technology, and supported by the National Natural Science Foundation of China (Grant Nos. 42088101 and 42030605), the National Key R&D Program of China (2018YFC1505602) and Natural Science Foundation of Jiangsu province (BK20191404). The authors thank ECMWF (https://cds.climate.copernicus.eu) for their providing the ERA5 reanalysis data. The monthly sea ice concentration and SST from 1979 to 2020 are obtained from the Met Office Hadley Centre (www.metoffice.gov.uk/hadobs/hadisst/data/download.html). The real time multivariate MJO index is available from the Australian Bureau of Meteorology (www.bom.gov.au/climate/mjo/graphics/rmm. 74toRealtime.txt).

ORCID iDs

Qian Lu https://orcid.org/0000-0003-3240-1098
Jian Rao https://orcid.org/0000-0001-5030-0288

References

Andrews D G, Holton J R and Leovy C B 1987 *Middle Atmosphere Dynamics* (New York: Academic Press)

Ayarzagüena B *et al* 2020 Uncertainty in the response of sudden stratospheric warmings and stratosphere-troposphere coupling to quadrupled CO_2 concentrations in CMIP6 models *J. Geophys. Res. Atmos.* **125** e2019JD032345

Ayarzagüena B, Barriopedro D, Garrido-Perez J M, Abalos M, Cámara A, García-Herrera R, Calvo N and Ordóñez C 2018 Stratospheric connection to the abrupt end of the 2016/2017 Iberian drought *Geophys. Res. Lett.* **45** 12639–46

Baldwin M P *et al* 2021 Sudden stratospheric warmings *Rev. Geophys.* **59** e2020RG000708

Baldwin M P and Dunkerton T J 1999 Propagation of the Arctic Oscillation from the stratosphere to the troposphere *J. Geophys. Res. Atmos.* **104** 30937–46

Baldwin M P and Dunkerton T J 2001 Stratospheric harbingers of anomalous weather regimes *Science* **294** 581–4

Baldwin M P and Thompson D W J 2009 A critical comparison of stratosphere–troposphere coupling indices *Q. J. R. Meteorol. Soc.* **1227** 496

Blackport R and Screen J A 2021 Observed statistical connections overestimate the causal effects of arctic sea ice changes on midlatitude winter climate *J. Clim.* **34** 3021–38

Butler A H, Lawrence Z D, Lee S H, Lillo S P and Long C S 2020 Differences between the 2018 and 2019 stratospheric polar vortex split events *Q. J. R. Meteorol. Soc.* **146** 3503–21

Butler A H, Seidel D J, Hardiman S C, Butchart N, Birner T and Match A 2015 Defining sudden stratospheric warmings *Bull. Am. Meteorol. Soc.* **96** 1913–28

Cao C, Chen Y, Rao J, Liu S, Li S and Ma M 2019 Statistical characteristics of major sudden stratospheric warming events in CESM1-WACCM : a comparison *Atmosphere* **10** 519

Charlton A J and Polvani L M 2007 A new look at stratospheric sudden warmings. Part I: climatology and modeling benchmarks *J. Clim.* **20** 449–69

De La Cámara A, Birner T and Albers J R 2019 Are sudden stratospheric warmings preceded by anomalous tropospheric wave activity? *J. Clim.* **32** 7173–89

Domeisen D I V, Garfinkel C I and Butler A H 2019 The teleconnection of El Niño southern oscillation to the stratosphere *Rev. Geophys.* **57** 5–47

Garfinkel C I, Feldstein S B, Waugh D W, Yoo C and Lee S 2012 Observed connection between stratospheric sudden warmings and the Madden-Julian oscillation *Geophys. Res. Lett.* **39** L18807

Hersbach H *et al* 2020 The ERA5 global reanalysis *Q. J. R. Meteorol. Soc.* **146** 1999–2049

Hu D and Guan Z 2018 Decadal relationship between the stratospheric Arctic vortex and pacific decadal oscillation *J. Clim.* **31** 3371–86

Hu J, Ren R and Xu H 2014 Occurrence of winter stratospheric sudden warming events and the seasonal timing of spring stratospheric final warming *J. Atmos. Sci.* **71** 2319–34

Hu Y 2020 The very unusual polar stratosphere in 2019–2020 *Sci. Bull.* **65** 1775–7

Karpechko A Y, Charlton-Perez A, Balmaseda M, Tyrrell N and Vitart F 2018 Predicting sudden stratospheric warming 2018 and its climate impacts with a multimodel ensemble *Geophys. Res. Lett.* **45** 13538–46

Karpechko A Y, Hitchcock P, Peters D H W and Schneidereit A 2017 Predictability of downward propagation of major sudden stratospheric warmings *Q. J. R. Meteorol. Soc.* **143** 1459–70

Kim B M, Son S W, Min S K, Jeong J H, Kim S J, Zhang X, Shim T and Yoon J H 2014 Weakening of the stratospheric polar vortex by Arctic sea-ice loss *Nat. Commun.* **5** 4646

Lee S H 2021 The January 2021 sudden stratospheric warming *Weather* **76** 135–6

Lee S H and Butler A H 2019 The 2018–2019 Arctic stratospheric polar vortex *Q. J. R. Meteorol. Soc.* **143** 1459–70

Liu S M, Chen Y H, Rao J, Cao C, Li S Y, Ma M H and Wang Y B 2019 Parallel comparison of major sudden stratospheric warming events in CESM1-WACCM and CESM2-WACCM *Atmosphere* **10** 679

Lu Q, Rao J, Guo D, Yu M and Yu Y 2021 Downward propagation of sudden stratospheric warming signals and the local environment in the Beijing-Tianjin-Hebei region: a comparative study of the 2018 and 2019 winter cases *Atmos. Res.* **254** 105514

Nishii K, Nakamura H and Miyasaka T 2009 Modulations in the planetary wave field induced by upward-propagating Rossby wave packets prior to stratospheric sudden warming events: a case-study *Q. J. R. Meteorol. Soc.* **135** 39–52

Overland J, Hall R, Hanna E, Karpechko A, Vihma T, Wang M and Zhang X 2020 The polar vortex and extreme weather: the beast from the east in winter 2018 *Atmosphere* **11** 664

Polvani L M and Waugh D W 2004 Upward wave activity flux as a precursor to extreme stratospheric events and subsequent anomalous surface weather regimes *J. Clim.* **17** 3548–54

Rao J and Garfinkel C I 2020 Arctic ozone loss in march 2020 and its seasonal prediction in cfsv2: a comparative study with the 1997 and 2011 cases *J. Geophys. Res. Atmos.* **125** e2020JD033524

Rao J and Garfinkel C I 2021a CMIP5/6 models project little change in the statistical characteristics of sudden stratospheric warmings in the 21st century *Environ. Res. Lett.* **16** 034024

Rao J and Garfinkel C I 2021b The strong stratospheric polar vortex in March 2020 in sub-seasonal to seasonal models: implications for empirical prediction of the low arctic total ozone extreme *J. Geophys. Res. Atmos.* **126** e2020JD034190

Rao J, Garfinkel C I, Chen H and White I P 2019a The 2019 new year stratospheric sudden warming and its real-time predictions in multiple S2S models *J. Geophys. Res. Atmos.* **124** 11155–74

Rao J, Garfinkel C I and White I P 2020a predicting the downward and surface influence of the February 2018 and January 2019 sudden stratospheric warming events in subseasonal to seasonal (S2S) models *J. Geophys. Res. Atmos.* **125** e2019JD031919

Rao J, Garfinkel C I, White I P and Schwartz C 2020b The Southern Hemisphere minor sudden stratospheric warming in September 2019 and its predictions in S2S models *J. Geophys. Res. Atmos.* **125** e2020JD032723

Rao J, Liu S and Chen Y 2021 Northern Hemisphere sudden stratospheric warming and its downward impact in four Chinese CMIP6 models *Adv. Atmos. Sci.* **38** 187–202

Rao J, Ren R, Chen H, Liu X, Yu Y, Hu J and Zhou Y 2019b Predictability of stratospheric sudden warmings in the beijing climate center forecast system with statistical error corrections *J. Geophys. Res. Atmos.* **124** 8385–400

Rao J, Ren R, Chen H, Yu Y and Zhou Y 2018 The Stratospheric Sudden Warming Event in February 2018 and its Prediction by a Climate System Model *J. Geophys. Res. Atmos.* **123** 13332–45

Rayner N A, Parker D E, Horton E B, Folland C K, Alexander L V, Rowell D P, Kent E C and Kaplan A 2003 Global analyses of sea surface temperature, sea ice, and night marine air temperature since the late nineteenth century *J. Geophys. Res.* **108** 4407

Screen J A 2017 Simulated atmospheric response to regional and pan-Arctic sea ice loss *J. Clim.* **30** 3945–62

Shen X, Wang L and Osprey S 2020 Tropospheric forcing of the 2019 Antarctic sudden stratospheric warming *Geophys. Res. Lett.* **47** e2020GL089343

Sun L, Deser C and Tomas R A 2015 Mechanisms of stratospheric and tropospheric circulation response to projected Arctic sea ice loss *J. Clim.* **28** 7824–45

Wheeler M C and Hendon H H 2004 An all-season real-time multivariate MJO index: development of an index for monitoring and prediction *Mon. Weather Rev.* **132** 1917–32